New Test of the Gravitational Inverse-Square Law at the Submillimeter Range with Dual Modulation and Compensation

Wen-Hai Tan,[1] Shan-Qing Yang,[1,*] Cheng-Gang Shao,[1] Jia Li,[1] An-Bin Du,[1] Bi-Fu Zhan,[2] Qing-Lan Wang,[3] Peng-Shun Luo,[1] Liang-Cheng Tu,[1] and Jun Luo[1,4,†]

[1]*MOE Key Laboratory of Fundamental Physical Quantities Measurements, School of Physics, Huazhong University of Science and Technology, Wuhan 430074, People's Republic of China*

[2]*School of Electrical and Electronic Engineering, Wuhan Polytechnic University, Wuhan 430000, People's Republic of China*

[3]*School of Science, Hubei University of Automotive Technology, Shiyan 442002, People's Republic of China*

[4]*Sun Yat-sen University, Guangzhou 510275, People's Republic of China*

(Received 17 August 2015; revised manuscript received 27 January 2016; published 30 March 2016)

By using a torsion pendulum and a rotating eightfold symmetric attractor with dual modulation of both the interested signal and the gravitational calibration signal, a new test of the gravitational inverse-square law at separations down to 295 μm is presented. A dual-compensation design by adding masses on both the pendulum and the attractor was adopted to realize a null experiment. The experimental result shows that, at a 95% confidence level, the gravitational inverse-square law holds ($|\alpha| \leq 1$) down to a length scale $\lambda = 59$ μm. This work establishes the strongest bound on the magnitude α of Yukawa-type deviations from Newtonian gravity in the range of 70–300 μm, and improves the previous bounds by up to a factor of 2 at the length scale $\lambda \approx 160$ μm.

DOI: 10.1103/PhysRevLett.116.131101

The four known fundamental forces in nature, gravity, electromagnetic interaction, weak, and strong interactions, are described by general relativity and the standard model, respectively. However, these two theories appear to be fundamentally incompatible. To connect gravity to the rest of physics, two of the most serious problems still exist: the hierarchy problem [1,2] and the cosmological constant problem [3–5]. Based on the ideas of string theory or M theory, a number of speculations have been proposed and predict a deviation from the gravitational inverse-square law (ISL) in a short-range regime [1–9]. Comprehensive reviews of such theories and predictions can be found in Ref. [8]. The deviations from the ISL are usually parametrized according to a Yukawa potential,

$$V(r) = -G\frac{m_1 m_2}{r}(1 + \alpha e^{-r/\lambda}), \tag{1}$$

where G is the Newtonian gravitational constant, α is the strength of any new interaction with a length scale of λ, and r is the separation between two masses. Motivated by these considerations, a large amount of experiments have been performed in the short range [10–24]. In this Letter we report a new test of the ISL using a torsion pendulum with separations down to 295 μm.

In torsion pendulum experiments for detecting the short-range ISL violation, the most straightforward way is to measure the variation of the force between two plane masses as their separation is modulated periodically. This method, as used in our previous experiments [23,24], has high sensitivity due to the fact that the total force is along the most sensitive direction of the pendulum, but its major disadvantage is that the signal frequency is identical to the drive frequency. An alternative method that separates the signal and disturbance frequencies was employed by the Eöt-Wash group [10], but the signal strength is reduced because only the transverse force is in the most sensitive direction. In our new design, the attractor is improved to be eightfold azimuthal symmetric, and rotates about a horizontal axis, as shown in Fig. 1. This design puts the signal frequency at the 8th harmonic of the rotation, far from the fundamental disturbance frequency, but allows the total Yukawa force to be detected in the most sensitive direction of the torsion pendulum.

An upgraded **I**-shaped pendulum with a mass of 59.693 g, is suspended facing to the eightfold attractor by a 70-cm-long, 25-μm-diameter tungsten fiber, as shown in Fig. 2(a). The middle part of the pendulum is a $61.491 \times 8.000 \times 12.000$ mm^3 (x-y-z) glass block, on each end of which two $14.630 \times 19.756 \times 27.138$ mm^3 glass bases (G_1, G_2) is attached symmetrically to make the test mass and the compensation mass protrude. Two $14.610 \times 0.200 \times 12.003$ mm^3 tungsten test masses (Wt_1, Wt_2) are first glued on two equal-area glass substrates (Gt_1, Gt_2) with a thickness of 0.486 mm, then the two substrates are glued on the higher part of the surface of the G_1 and G_2, respectively. On the lower part of the G_1 and G_2, two $14.610 \times 0.289 \times 12.003$ mm^3 gravitational compensation pieces (Wtc_1, Wtc_2) are adhered below each test mass, which are used to cancel the change of the Newtonian force. A special glass clamp is attached on top of the middle glass block to guide the suspended fiber to the center of the pendulum with an uncertainty of 5 and 6 μm in the x and y directions, respectively.

The attractor consists of 8 tungsten source masses (Ws_i, $i = 1, 2, \ldots 8$, similarly hereinafter) and 8 tungsten compensation masses (Wc_i) that are arrayed alternatively on a 100-mm-diameter, 3-mm-thick glass disk. The centers of the 16 masses rests periodically on a 38.80-mm-radius circle. Each source mass, with dimensions $17.597 \times 0.200 \times 11.403$ mm^3, is first adhered to a 0.420-mm-thick glass substrate (Gs_i) with the same area, then the 8 substrates are glued to the glass disk with eightfold azimuth symmetry. Similarly, eight $17.597 \times 0.219 \times 11.403$ mm^3 compensation masses are glued on the disk alternately. To keep the surface of the attractor at the same level, eight equal-area but 0.395-mm-thick glass substrates (Gc_i) are used to cover each Wc_i. All assembly processes were guided by an optical image measuring instrument. The position and the azimuth are aligned within 20 μm and 1 mrad in accuracy, respectively.

At separation of 295 μm, the Newtonian torque between one test mass and one source mass is $\sim 1.5 \times 10^{-14}$ N · m, about 3000 times larger than the expected sensitivity. Therefore, if we want to keep the change of the Newtonian torque below the sensitivity, the uncertainty of the thickness of the masses should be less than 0.1 μm, which is very difficult to achieve in fabrication. The problem was solved by adding compensation masses on both the pendulum and the attractor (we name it "dual compensation"); thus, a "null" experiment design was realized. The change of the Newtonian torque is cancelled to be $< 1.5 \times 10^{-17}$ N · m at the 8th harmonic with a larger span of the separation (from $\sim$100 μm to several mm). However, because both the compensation masses on the pendulum and the attractor are about 0.4 mm back inside with respect to the test masses and the source masses, respectively, the expected change of the Yukawa torque should not be suppressed due to the faster decay of this force with separation, as shown in Fig. 2(b). The dual compensation design reduces the accuracy requirements of the geometric dimensions and the alignment about 10 times.

To realize a null experiment, all the components were elaborately ground, polished, and assembled as described in Refs. [23,24]. As shown in Fig. 1, the attractor disk, adhered to an aluminum shaft with a precise bearing, and the alignment glass block are all mounted on the same platform of the 6-degree-of-freedom stage. The relative positions between the alignment glass, the attractor, and the shaft (rotation axis) were measured by a coordinate measuring machine during the assembly. By moving the alignment glass to touch the pendulum in the vacuum chamber, the attractor rotation axis was aligned with the center of the pendulum within 4 and 7 μm in the x and z directions, respectively. Similarly, the error of the separation between the pendulum and the attractor (in the y direction) was measured to be less than 6 μm. The attractor disk was rotated at a uniform velocity ω_d. The attitude of the attractor was monitored by an autocollimator and adjusted to be parallel to the pendulum within 42 μrad. The run-out and the wobble of the attractor were determined using an infrared optical instrument [25] and an autocollimator to be less than 4.5 nm and 0.25 μrad at $8\omega_d$, respectively. The initial azimuthal angle of the attractor relative to the pendulum was adjusted within 0.5° uncertainty, which keeps the expected Yukawa signal in phase with $\sin(8\omega_d t)$. After considering all the errors, the $8\omega_d$ Newtonian torque at the separation of 295 μm was calculated to be $\tau_{Ni} = (0.7 \pm 0.5) \times 10^{-17}$ N · m for the in-phase component, and $\tau_{Nq} = (-0.1 \pm 0.5) \times 10^{-17}$ N · m for the quadrature one [as shown in Fig. 2(b)]. The main errors of the Newtonian torque at $8\omega_d$ are shown in Table I. Similarly, the uncertainty of the Yukawa torque that caused by the geometric parameters is estimated by numerical integration with different α and λ, which is $\leq 8\%$ with $70 \leq \lambda \leq 300$ μm, and has been combined in the constraint on the Yukawa violation.

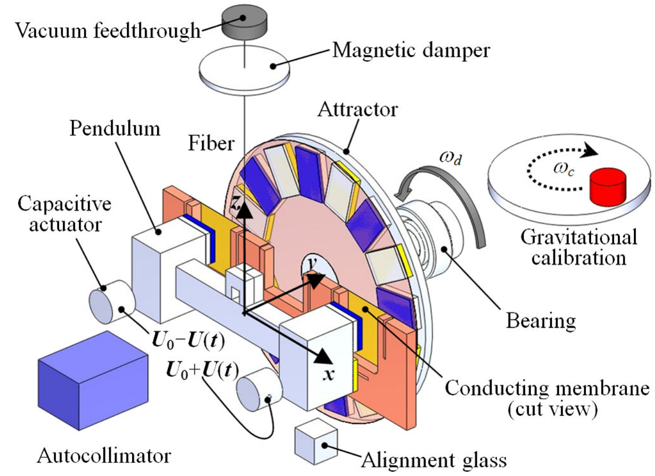

FIG. 1. Schematic drawing of the experimental setup (not to scale). The attractor and the alignment glass are mounted on a 6-degree-of-freedom stage (not shown here). A rotary stage outside the vacuum chamber is used to rotate the attractor through a feedthrough. The pendulum twist is measured by an autocollimator, and controlled by two differential capacitive actuators. The sensitivity of the pendulum is calibrated synchronously by rotating a copper cylinder outside the vacuum chamber.

Three procedures were used to minimize the electrostatic force between the pendulum and the attractor. (i) The pendulum and the attractor were all gold coated and grounded. An additional 10-μm-thick BeCu foil covered the attractor's surface to make the charge distribution uniform. (ii) Facing to the test masses, two tightly stretched 30-μm-thick BeCu conducting membranes were inserted between the pendulum and the attractor to prevent direct electrostatic coupling. (iii) The potential differences between the pendulum and the two membranes were determined and compensated individually for each data run, as described in Ref. [23].

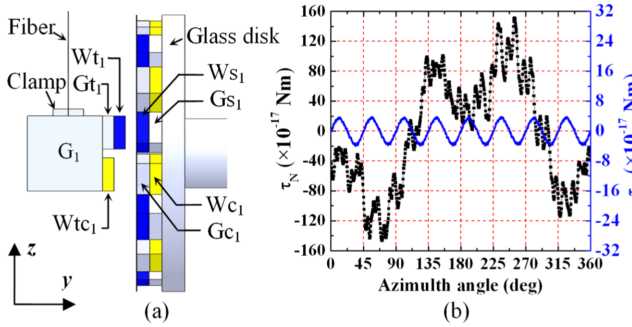

FIG. 2. (a) The front view of the bilateral symmetric pendulum and the eightfold attractor. (b) The residual Newtonian torque τ_N (dotted line) and the expected Yukawa torque τ_Y (solid line), which are calculated from the geometric parameters of the masses with the separation of 295 μm. The Yukawa torque changes as a sinusoidal curve with a frequency of $8\omega_d$ and an amplitude of 3.4×10^{-17} N · m ($\alpha = 0.12$, $\lambda = 0.1$ mm are used according to the previous bound [10]). The residual Newtonian torque varies mainly at the fundamental frequency due to the eccentricity of the attractor. From the Fourier transform, the $8\omega_d$ Newtonian torque is $(0.7 \pm 0.5) \times 10^{-17}$ N · m (the in-phase) and $(-0.1 \pm 0.5) \times 10^{-17}$ N · m (the quadrature), respectively.

The entire system was installed inside a vacuum chamber maintained at a pressure of approximately 10^{-5} Pa by an ion pump. During short range force detection, the pendulum-membrane separation is set to ~200 μm. A proportional-integral-differential electrostatic feedback system [23] was used to keep the pendulum at a fixed position. The sensitivity

TABLE I. Main error sources of the $8\omega_d$ Newtonian torques (with 1σ).

Main error sources	Measured values	$\delta(\Delta\tau)$ ($\times 10^{-17}$ N · m)	
Pendulum			0.18
thickness of Wt	0.200 (1) mm	$0.07 \times \sqrt{2}$	
Position z of Wt	7.580 (7) mm	$0.04 \times \sqrt{2}$	
Thickness of Wtc	0.289 (1) mm	$0.05 \times \sqrt{2}$	
Position z of Wtc	−7.557 (7) mm	$0.04 \times \sqrt{2}$	
Adhesive	0.0009 (10) g	$0.04 \times \sqrt{6}$	
Others		0.04	
Attractor			0.13
Thickness of Ws	0.200 (1) mm	$0.03 \times \sqrt{8}$	
Position y of Ws	−0.527 (2) mm	$0.02 \times \sqrt{8}$	
Thickness of Wc	0.219 (1) mm	$0.02 \times \sqrt{8}$	
Others		0.06	
Alignments	≤ 7 μm and ≤ 42 μrad		0.09
Run-out	≤ 4.5 nm		0.34
Wobble	≤ 0.25 μrad		0.27
Initial phase	$\leq 0.5°$		0.05
Total [a]			**0.50**

[a]This amplitude error is treated as both the in-phase and the quadrature component errors, because the initial phases of the run-out and wobble of the attractor disk were not determined deliberately.

of the closed-loop pendulum was calibrated synchronously by a 1140 g copper cylinder rotating at a frequency of $\omega_c (= 15.7079$ mrad/s). The amplitude of the calibration signal was first determined in the free oscillation mode of the torsion pendulum with the pendulum-membrane separation of ~4 mm for negligible electrostatic disturbance. The response of the torsion pendulum is $\theta(\omega_c) = \tau(\omega_c)/\sqrt{I^2(\omega_0^2 - \omega_c^2)^2 + (I\omega_0^2/Q)^2}$, with the pendulum's moment of inertia $I = (6.977 \pm 0.002) \times 10^{-5}$ kg m^2, the free oscillation frequency $\omega_0 = (10.74 \pm 0.04)$ mrad/s, and the quality factor $Q \sim 2500$. The twist of the pendulum at ω_c is $\theta_c = (71.3 \pm 1.6)$ nrad, so the gravitational calibration torque is accordingly determined as $\tau_c = (65.6 \pm 2.1) \times 10^{-17}$ N · m.

In the closed-loop system, the feedback voltages $U_0 + U(t)$ and $U_0 - U(t)$ are applied on two electrodes, respectively, with $U_0 = 5$ V. The equation of motion of the closed-loop torsion pendulum is

$$I\ddot{\theta} + k(1 + i/Q)\theta - k_e\theta = \tau(t) - \beta U(t), \tag{2}$$

where k_e is the electrostatic coupling coefficient between the pendulum and the membrane, $\tau(t)$ is the total external torque, and β is the ratio of the control torque to the feedback voltage $U(t)$. $U(t)$ is calculated as $U(t) = k_p\theta + k_d\dot{\theta} + k_i \int \theta dt$, with $k_p = 0.18$ V/μrad, $k_i = 0.0001$ V/(μrad · s), and $k_d = 9.0$ V/(μrad · s^{-1}). The measured torque τ at the frequency ω [denoted as $\tau(\omega)$] is calculated according to the transfer function derived from Eq. (2) as

$$H_U(\omega) \equiv \frac{U(\omega)}{\tau(\omega)} = \frac{U(\omega)}{\theta(\omega)}\frac{\theta(\omega)}{\tau(\omega)} = \frac{\frac{1/I}{i\omega T_F + 1}[k_p + \frac{k_i}{i\omega} + \frac{i\omega k_d}{i\omega T_f + 1}]}{(\omega_0^2 - \frac{k_e}{I} - \omega^2) + i\frac{\omega_0^2}{Q} + \frac{\beta/I}{i\omega T_F + 1}[k_p + \frac{k_i}{i\omega} + \frac{i\omega k_d}{i\omega T_f + 1}]}, \tag{3}$$

where $T_F = 10$ and $T_f = 4$ s, are the time constants of the lowpass filter of the θ and $\dot{\theta}$. The parameters, $k_e = (2 \pm 6) \times 10^{-9}$ N · m/rad and $\beta = (4.7 \pm 0.3) \times 10^{-13}$ N · m/V, are deduced from the response of the feedback voltage U_c on the known gravitational calibration signal τ_c.

The rotating frequency ω_d of the attractor was set to 1.63364 mrad/s, so that the interested signal frequency $\omega_s (= 8\omega_d)$ is at the low noise frequency band. Each data set, including the outputs of the autocollimator, the feedback voltage $U(t)$, and five temperature sensors, were recorded at a sampling rate of 1 Hz for about 5 days. Between the data sets, the drift of the equilibrium position of the pendulum was adjusted, and the potential differences between the pendulum and the two membranes were remeasured and compensated. The $8\omega_d$ feedback voltage signal $U(\omega_s)$ is extracted by $(2/T)\int_0^T U(t)\cos(\omega_s t)dt$ and

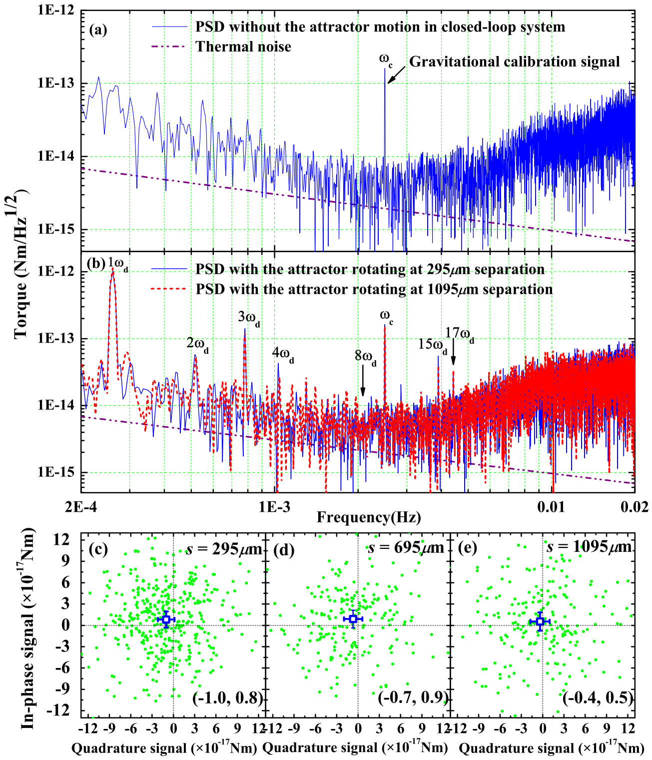

FIG. 3. (a) The typical torque PSD of the pendulum with the attractor at rest. It is closed to the thermal noise limit at ~mHz, but increased at higher frequency due to the readout noise. (b) Comparison of the torque PSDs of the pendulum with the attractor rotating at separations of 295 and 1095 μm. Both of them have a similar structure in the full frequency range. No significant signals appear at $8\omega_d$. The obvious signals at $1\omega_d - 4\omega_d$ are caused by both the Newtonian torque and the disturbance of the shield membrane, and the $15\omega_d$ and $17\omega_d$ signals are Newtonian torques due to the imperfect assembly of the attractor. (c)–(e) The measured torques at $8\omega_d$ at 295, 695, and 1095 μm separations, respectively. Each solid dot represents a value obtained from a 5-rotation-period data segment, and the squares represent the mean values (shown in brackets) with 2σ error.

$(2/T)\int_0^T U(t)\sin(\omega_s t)dt$, so does the calibration signal $U(\omega_c)$. According to Eq. (3), the measured torque $\tau(\omega_s)$ is calculated as $\tau(\omega_s) = [U(\omega_s)/H_U(\omega_s)] = [U(\omega_s)/U(\omega_c)]$ $[H_U(\omega_c)/H_U(\omega_s)]\tau_c(\omega_c)$, where $|H_U(\omega_c)/H_U(\omega_s)| = 1.043(5)$, and its error caused by k_e and β are common mode, so have been canceled greatly.

The typical power spectrum density (PSD) with and without the rotation of the attractor are shown in Figs. 3(a)–3(b). At the 295 μm separation, the ISL was tested with a duration of about 80 days. After subtracting the tiny residual Newtonian torque calculated above, the measured signal at $8\omega_d$ is shown in Fig. 3(c), and the in-phase signal τ_i and the quadrature signal τ_q with 1σ error are

$$\tau_i = (0.8 \pm 0.3_{\text{stat}} \pm 0.5_{\text{syst}}) \times 10^{-17}\ \text{N} \cdot \text{m}, \quad (4)$$

$$\tau_q = (-1.0 \pm 0.3_{\text{stat}} \pm 0.5_{\text{syst}}) \times 10^{-17}\ \text{N} \cdot \text{m}, \quad (5)$$

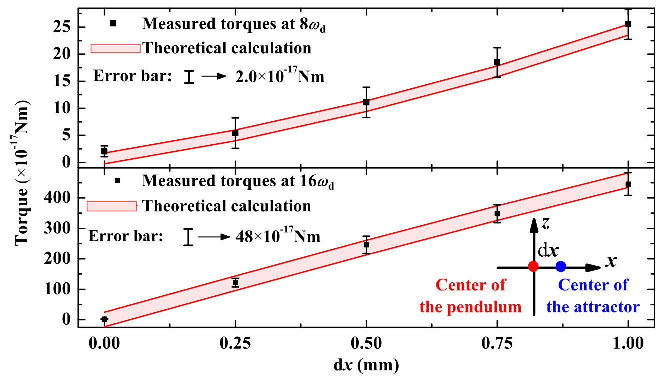

FIG. 4. Non-null experimental results of the $8\omega_d$ (upper) and $16\omega_d$ (lower) Newtonian torque. The shaded belt represents the theoretical calculations, and the little squares are the measured values, both with 2σ error. The $8\omega_d$ theoretical Newtonian torque shows a smaller error bar compared with the $16\omega_d$ one due to the dual compensation design. Inset: schematic drawing of the displacement of the attractor with respect to the pendulum.

where the first uncertainty is statistic, and the second is the systematic uncertainty that mainly contributed by the residual Newtonian torque errors. The result shows that at the 2σ level the gravitational ISL still holds.

To distinguish the systematic effects from electrostatic or other disturbances due to the shield membrane, two additional experiments with lager separations of 695 and 1095 μm were conducted. Each experiment lasted about 50 days. In the two additional experiments, the pendulum-membrane separations were kept the same as that in the 295-μm-separation experiment, which ensures the disturbance from the membrane identical, but the Yukawa effect is negligible due to the larger separation. The comparison of the torque PSDs of the pendulum at separations of 295 and 1095 μm is shown in Fig 3(b). After subtracting the slightly increased Newtonian torque of $(1.3 \pm 0.5) \times 10^{-17}\ \text{N} \cdot \text{m}$, the results are consistent with that of the 295-μm-separation experiment at the 2σ level, shown in Figs. 3(c)–3(e). The additional experiments indicate that the disturbance from the shield membrane does not significantly increase the error in the 295-μm-separation experiment.

Furthermore, several "non-null" experiments were performed to verify the reliability. By deliberately shifting the attractor and the pendulum along the x direction, the $8\omega_d$ and $16\omega_d$ Newtonian torques are expected to increase significantly. These characteristic signals allow us to confirm that the instrument is performing properly. Experiments with $dx = 0.250(6)$, 0.500(6), 0.750(6), and 1.000(6) mm were carried out. The results (shown in Fig. 4) generally represent a consistency with the Newtonian torques calculated with the measured geometric parameters, which provide an additional check on the design and installation of the whole experimental system.

Constraint on the Yukawa interaction at a 95% confidence level is set by the in-phase signal τ_i of the 295-μm separation

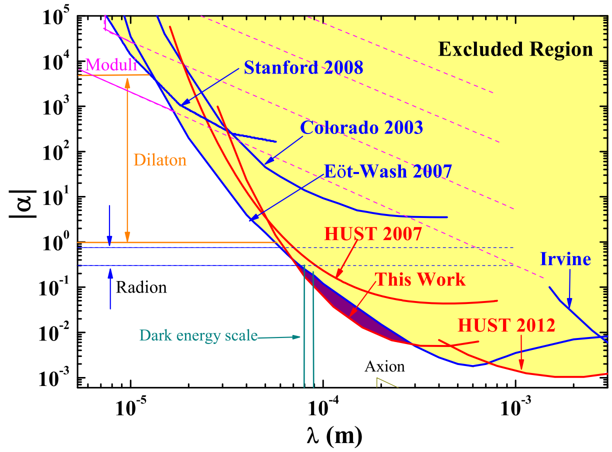

FIG. 5. Constraints on Yukawa violation of the Newtonian $1/r^2$ law. The shaded region is excluded at a 95% confidence level. The heavy lines labeled Stanford 2008 [13], Colorado 2003 [14], Eöt-Wash 2007 [10], HUST 2007 and 2012 [23,24], This work, and Irvine [11] show the experimental constraints, respectively. Light lines show various theoretical predictions summarized in Ref. [8].

experiment as $2 \times \sqrt{0.8^2 + 0.3^2 + 0.5^2} = 2.0 \times 10^{-17}$ N·m. This result sets the strongest bound on α in the range of 70–300 μm, as shown in Fig. 5. At the length of $\lambda \approx 160$ μm, we improve the previous bounds by up to a factor of 2, and the inverse-square law holds ($|\alpha| \leq 1$) down to a length scale $\lambda = 59$ μm. For the two large extra-dimension scenarios with $\alpha = 16/3$ [8], the experiment requires the unification mass $M_* \geq 2.8$ TeV$/c^2$ with the size $R_* \leq 47$ μm, agreeing with our previous result [23]. The main limit of the present sensitivity is the disturbance of the vibration of the shield membrane, which also restricts the minimal accessible separation.

We thank Riley Newman, Ho Jung Paik, and Vadim Milyukov for helpful discussion. This work was supported by the National Basic Research Program of China under Grant No. 2010CB832802, the National Natural Science Foundation of China under Grants No. 91436212, 11325523, No. 11305057, and No. 11475066.

*ysq2011@hust.edu.cn
†junluo@mail.hust.edu.cn

[1] N. Arkani-Hamed, S. Dimopoulos, and G. Dvali, Phys. Lett. B **429**, 263 (1998); Phys. Rev. D **59**, 086004 (1999).
[2] S. Dimopoulos and G. F. Giudice, Phys. Lett. B **379**, 105 (1996).
[3] S. R. Beane, Gen. Relativ. Gravit. **29**, 945 (1997).
[4] R. Sundrum, J. High Energy Phys. 07 (1999) 001; Phys. Rev. D **69**, 044014 (2004).
[5] D. B. Kaplan and M. B. Wise, J. High Energy Phys. 08 (2000) 037.
[6] N. Arkani-Hamed, S. Dimopoulos, G. Dvali, and N. Kaloper, Phys. Rev. Lett. **84**, 586 (2000).
[7] L. Randall and R. Sundrum, Phys. Rev. Lett. **83**, 4690 (1999).
[8] E. G. Adelberger, B. R. Heckel, and A. E. Nelson, Annu. Rev. Nucl. Part. Sci. **53**, 77 (2003); E. G. Adelberger, J. H. Gundlach, B. R. Heckel, S. Hoedl, and S. Schlamminger, Prog. Part. Nucl. Phys. **62**, 102 (2009).
[9] E. G. Adelberger, B. R. Heckel, S. Hoedl, C. D. Hoyle, D. J. Kapner, and A. Upadhye, Phys. Rev. Lett. **98**, 131104 (2007).
[10] C. D. Hoyle, D. J. Kapner, B. R. Heckel, E. G. Adelberger, J. H. Gundlach, U. Schmidt, and H. E. Swanson, Phys. Rev. D **70**, 042004 (2004); D. J. Kapner, T. S. Cook, E. G. Adelberger, J. H. Gundlach, B. R. Heckel, C. D. Hoyle, and H. E. Swanson, Phys. Rev. Lett. **98**, 021101 (2007).
[11] J. K. Hoskins, R. D. Newman, R. Spero, and J. Schultz, Phys. Rev. D **32**, 3084 (1985).
[12] R. S. Decca, D. López, H. B. Chan, E. Fischbach, D. E. Krause, and C. R. Jamell, Phys. Rev. Lett. **94**, 240401 (2005); Y.-J. Chen, W. K. Tham, D. E. Krause, D. López, E. Fischbach, and R. S. Decca, arXiv:1410.7267.
[13] J. Chiaverini, S. J. Smullin, A. A. Geraci, D. M. Weld, and A. Kapitulnik, Phys. Rev. Lett. **90**, 151101 (2003); A. A. Geraci, S. J. Smullin, D. M. Weld, J. Chiaverini, and A. Kapitulnik, Phys. Rev. D **78**, 022002 (2008).
[14] J. C. Long, H. W. Chan, A. B. Churnside, E. A. Gulbis, M. C. M. Varney, and J. C. Price, Nature (London) **421**, 922 (2003).
[15] M. Masuda and M. Sasaki, Phys. Rev. Lett. **102**, 171101 (2009).
[16] S. K. Lamoreaux, Phys. Rev. Lett. **78**, 5 (1997); A. O. Sushkov, W. J. Kim, D. A. R. Dalvit, and S. K. Lamoreaux, *ibid.* **107**, 171101 (2011).
[17] M. Bordag, U. Mohideen, and V. M. Mostepanenko, Phys. Rep. **353**, 1 (2001); G. L. Klimchitskaya, U. Mohideen, and V. M. Mostepanenko, Phys. Rev. D **87**, 125031 (2013).
[18] Y. Kamiya, K. Itagaki, M. Tani, G. N. Kim, and S. Komamiya, Phys. Rev. Lett. **114**, 161101 (2015).
[19] M. V. Moody and H. J. Paik, Phys. Rev. Lett. **70**, 1195 (1993).
[20] R. D. Newman, E. C. Berg, and P. E. Boynton, Space Sci. Rev. **148**, 175 (2009).
[21] J. C. Long and V. A. Kostelecký, Phys. Rev. D **91**, 092003 (2015).
[22] C.-G. Shao, Y.-J. Tan, W.-H. Tan, S.-Q. Yang, J. Luo, and M. E. Tobar, Phys. Rev. D **91**, 102007 (2015).
[23] L.-C. Tu, S.-G. Guan, J. Luo, C.-G. Shao, and L.-X. Liu, Phys. Rev. Lett. **98**, 201101 (2007).
[24] S.-Q. Yang, B.-F. Zhan, Q.-L. Wang, C.-G. Shao, L.-C. Tu, W.-H. Tan, and J. Luo, Phys. Rev. Lett. **108**, 081101 (2012).
[25] L.-C. Tu, Q. Li, Q.-L. Wang, C.-G. Shao, S.-Q. Yang, L.-X. Liu, Q. Liu, and J. Luo, Phys. Rev. D **82**, 022001 (2010).